Journal of the Korean Physical Society (2023) 83:620–633
https://doi.org/10.1007/s40042-023-00839-1

Online ISSN 1976-8524
Print ISSN 0374-4884

ORIGINAL PAPER - PARTICLES AND NUCLEI

Overview of fusion-like neutron sources based on high-intensity linear accelerators

Yoo Lim Cheon[1] · Hyun Wook Kim[1] · Emre Cosgun[2] · Moses Chung[2]

Received: 1 February 2023 / Revised: 15 March 2023 / Accepted: 15 March 2023 / Published online: 12 June 2023

Abstract
A dedicated linear accelerator for continuous wave (CW) D^+ beams to generate fusion-like neutrons is crucial for the breeding blanket module tests and fusion material irradiation experiments. In this article, we introduce the world-wide activities for such accelerator facilities. Then, we present the case study, pre-conceptual design, and major component specification overview for developing a linear accelerator that could provide the modest beam parameters (40 MeV, maximum 10 mA CW) for breeding module tests. We look into the specifications of the facility and prepare a layout of the envisioned accelerator, which could be aligned with the Korean domestic fusion program. We also carry out the preliminary beam dynamics/optics calculations and operation scenario development.

Keyword Linear accelerator · Nuclear fusion · Neutron source · Breeding blanket

1 Introduction

Many technical achievements have been reported in nuclear fusion science and technology in recent years [1]. For example, a private US fusion company, Commonwealth Fusion Systems (CFS), developed a prototype 20 T high-temperature-superconducting (HTS) magnet for a compact fusion reactor, and raised more than $1.8 billion in funding to commercialize its concept. International efforts to build and operate the International Thermonuclear Experimental Reactor (ITER) are also moving steadily despite many technical hurdles and construction cost escalation. Korean domestic fusion program based on KSTAR is making considerable contribution to the worldwide fusion community as well. The KSTAR team discovered a sustained high-temperature fusion plasma regime facilitated by fast ions [2], which opens the new door towards commercial fusion reactors.

Nevertheless, to realize fusion reactors, a handful of technical challenges remain to be overcome. Fusion community identified eight core technologies for ITER-type large scale tokamak. These include (1) core plasma control, (2) breeding blanket, (3) fusion materials, (4) fuel cycle, (5) divertor, (6) heating and current drive, (7) superconducting magnet, and (8) safety and licensing. The technology items (1), (6), and (7) deal with tokamak plasmas, whereas other items are associated with reactor engineering and neutronics.

It is worthwhile to note that fusion reactors and particle accelerators share various common technologies. For example, HTS magnets are getting more attention in the accelerator community in the context of future circular collider. A neutral beam injector is nothing but an electrostatic accelerator with negative ion sources. Heating and current drive devices require stable and high-power RF sources such as klystron, tetrode, and solid-state power amplifier, which are also key elements for RF acceleration of charged particles.

Emre Cosgun has contributed equally to this work.

✉ Moses Chung
mchung@unist.ac.kr

Yoo Lim Cheon
cylim2@kfe.re.kr

[1] Korea Institute of Fusion Energy, Daejeon 34133, Republic of Korea

[2] Department of Physics, Ulsan National Institute of Science and Technology, Ulsan 44919, Republic of Korea

2 Fusion-like neutron sources

One of the important areas where fusion meets accelerator technology is the generation of fusion-like neutrons using high-intensity accelerators. To test blanket and divertor under fusion-like environment, fusion community has demanded sources of neutrons with similar characteristics as those generated by D-T fusion reaction [3, 4]. Among various options, a concept based on acceleration of deuteron beam on the order of 100 mA to about 40 MeV followed by liquid-lithium target has been pursued since mid 1970 s. Fusion-relevant neutron has energy spectrum centered around 14.1 MeV, and provides He production rate of the order of ∼10 appm/dpa (atomic parts per million/displacements per atom). Transmuted gaseous He would make significant impacts on mechanical properties of fusion materials. Fission reactors cannot yield neutrons of such characteristics.

In mid-1970 s, the Fusion Materials Irradiation Test (FMIT) project was proposed in the US based on continuous wave (CW) high-current linear accelerators (linacs). To meet the average beam current on the order of 100 mA, CW operation was preferred but the super-conducting RF technology was not yet available at that time. Since mid-1990 s, the fusion community has reached a consensus on the International Fusion Materials Irradiation Facility (IFMIF) concept. The IFMIF aims to generate a neutron flux of 10^{18} n$/m^2/s$ and be capable of a total dose of ∼ 100 dpa. The IFMIF will be composed of two parallel linacs of deuteron beams. Each linac consists of an electron cyclotron resonance (ECR) ion source, four-vane RFQ, and superconducting half-wave resonator (HWR) cavities, producing 40 MeV final energy with 125 mA CW current. To test the feasibility of this high-power accelerator system and to minimize technical risks, the Linear IFMIF Prototype Accelerator (LIPAc) program is undergoing in Japan. The cost of the IFMIF would be no less than those of Spallation Neutron Source (SNS) project in US and European Spallation Source (ESS) in EU.

The recent trend in the fusion community is a staged approach to IFMIF [5]. By focusing only on DEMO needs, the requirements for the neutron flux are considerably reduced (max 20 dpa initially, followed by max 50 dpa in a second phase). Therefore, construction of approximately half the size of the IFMIF is being considered as the first phase. For example, European countries plan to build IFMIF-DONES (DEMO oriented neutron source), and Japan considers construction of Advanced Fusion Neutron Source (A-FNS) in Rokkasho. US is planning a Fusion Prototypic Neutron Source (FPNS), which could be constructed in the near term at moderate cost with accelerator parameters similar to IFMIF-DONES. More detailed cost estimates are expected soon. Whereas it is not originally intended for fusion material research, the MYRRHA project in Belgium can also be applied for fusion materials irradiation as its first phase program.

3 Activities in Korea

In Korea, there has been no coordinated effort toward fusion-relevant neutron sources. Some of the recent scattered activities are briefed here. In 2013, a workshop on IFMIF was held at Pohang Accelerator Laboratory, in which a discussion on the role of the Korean fusion community in the IFMIF/Engineering Validation and Engineering Design Activities (EVEDA) program was made. Around 2016, Busan International Fusion Neutron Source (BIFNS) concept was proposed based on high current RF ion source for deuteron or triton beams. At Korea Atomic Energy Research Institute (KAERI), the possibility to use multiple cyclotrons for fusion material and blanket R &D was investigated. Together with Pukyong National University, KAERI also developed a research program to apply its ion irradiation test facility (KAHIF) for emulating effects of fusion neutrons by ion beams.

Recently, the Korea Institute of Fusion Energy (KFE) performed a pre-conceptual design study for the Integrated Breeding Test Facility (IBTF) [6, 7]. In this facility, various critical aspects of breeding blanket would be evaluated such as tritium production and recovery, heat extraction, and structural integrity in a fusion-like environment. The IBFT will use the 40 MeV deuteron beam with a maximum CW average current of 10 mA. The 40 MeV deuteron interacts with a solid Beryllium (Be) target to produce fusion-like neutrons. The accelerator option for the IBTF would be finalized considering technology readiness, cost estimation, operation scenario, etc. In any case, such a dedicated breeding blanket test facility based on a moderate-intensity D^+ accelerator would play a key role for domestic fusion engineering programs similar to the KSTAR has done for fusion plasma science.

There are several neutron production targets in the domestic accelerator facilities. The Korea Multipurpose Accelerator Complex (KOMAC) produces neutrons using 100 MeV proton linac and beam dump as a neutron converter. The heavy ion accelerator RAON is equipped with nuclear data production system composed of a thick carbon target for white neutron and a thin lithium target for mono-energy neutrons. Nevertheless, those accelerators are basically user facilities, thus space, infrastructure, and beam times are not available for dedicated fusion materials irradiation or tritium breeding module tests. Furthermore, the average beam currents are limited to 1.6 mA for KOMAC and 1

mA for RAON, which are too low for evaluating long-term neutron irradiation effects.

4 Case study for deuteron accelerator unit

In this section, we first investigate the detailed specifications of linacs for generating fusion-like neutrons, which are now operational, under construction, or under planning over the world. Considering high average beam current required for the deuteron accelerator unit (DAU) of the KFE's proposed IBTF, we focus mainly on the linac not cyclotron option. In particular, we will introduce GANIL-SPIRAL2 in France [8–10], SARAF-PHASE2 in Israel [11, 12], IFMIF in Japan-EU [13, 14], IFMIF-DONES in Europe (Spain) [15], and Compact Material Irradiation Facility (CMIF) in China [16]. One of these types of accelerators could be a prototype for the DAU of the IBTF. The comparison of the beam specifications is shown in Table 1. Deuteron beam (D^+) is typically used to generate high energy neutrons including nuclear fusion-like mono-energetic neutrons (14.1 MeV) when it hits a target. The detailed target specifications in different accelerator facilities are shown in Table 2.

GANIL-SPIRAL2 and SARAF-PHASE2 are the user facilities that accelerate H^+ and D^+ (or Heavy ions) in both CW (Continuous Wave) and pulsed modes. They are using super-conducting linac technology to accelerate deuteron beam up to 200 kW (40 MeV, 5 mA) and will be utilized for the various kinds of nuclear physics experiments. The GANIL-SPIRAL2 uses a thick Carbon target in a rotating wheel converter and generates over 10^{17} $n/m^2/s$ flux of neutrons by 200 kW power of deuteron beams. Then the generated neutrons hit a Uranium Carbide (UCx) target, which produces radioactive neutron-rich Rare Isotope Beams (RIBs) up to 10^{14} fissions/s [8, 17]. The SARAF-PHASE2 uses Liquid Lithium (LiLiT) target to generate thermal neutrons, which will hit a secondary target for the purpose of nuclear physics research by using the exotic isotopes [18, 19].

IFMIF [20] and IFMIF-DONES [15] are the accelerator facilities dedicated for the fusion material irradiation tests, which accelerate deuteron beams up to 5 MW (40 MeV, 125 mA) in CW mode; the IFMIF has two linacs in parallel, so that total 10 MW of deuteron beam power is applied. The accelerated beams hit a LiLiT target (25 mm in thickness) to finally achieve a high structural damage (20 ∼ 50 dpa) irradiation induced by neutrons. A rectangular flat top beam profile on the target is highly required for the material irradiation tests. It can be achieved by using multipole magnets (e.g., octupoles, duodecapoles etc.), and the arrangement of quadrupole magnets before the target [21, 22]. As shown in Table 2, the beam footprint on a LiLiT target of IFMIF is 5 cm × 20 cm, and IFMIF-DONES is planning to cover a range from 5 cm × 10 cm to 5 cm × 20 cm with uniform densities.

The CMIF is developing a granular/powdery flow/jet target with a very small beam spot in order to increase the neutron flux and achieve over 50 dpa irradiation tests as a complementary approach to the IFMIF [23].

In KFE, a pre-conceptual design study has been initiated to construct a deuteron-beam-dedicated linac in Korea for the breeding blanket module tests. Our target beam specification is decided to be 20 MeV/u (40 MeV, deuteron) energy and 10 mA maximum beam current (total 400 kW of beam

Table 1 Comparison of the beam specifications for generating neutrons by using linear accelerators over the world

Facility	Beam type	Beam energy (MeV)	Beam current (mA)	Beam power (MW)
GANIL-SPIRAL2 (France)	H^+, D^+, $A/Q > 3$ (CW or Pulsed)	40	5	0.2
SARAF-PHASE2 (Israel)	H^+, D^+ (CW or Pulsed)	40	5	0.2
IFMIF (EU-JP)	D^+ (CW)	40	125 × 2	5 × 2
IFMIF-DONES (Europe)	D^+ (CW)	40	125	5
CMIF (China)	D^+ (CW)	50	10	0.5

Table 2 Comparison of the target specifications for generating neutrons by using linear accelerators over the world

Facility	Target type	Beam spot at target
GANIL-SPIRAL2 (France)	Carbon converter	∼10 cm^2
SARAF-PHASE2 (Israel)	LiLiT	∼2 cm^2
IFMIF (EU-JP)	LiLiT	5 cm × 20 cm
IFMIF-DONES (Europe)	LiLiT	5 cm × 10 cm, 5 cm × 20 cm
CMIF (China)	Granular flow Be	5 mm × 15 mm

power) in CW mode. The accelerated deuteron beam will hit a solid Be target of 20 cm × 20 cm spot size. We have mainly benchmarked the SARAF-PHASE2 facility from the injector to super-conducting linac section. Also, we investigated the main components of HEBT line based on IFMIF/IFMIF-DONES and studied in detail for making a rectangular shaped beam with 20 cm × 20 cm cross section in transverse space by using octupole magnets. The accelerated beam should have a uniform distribution on target with less than 5% of the flat top uniformity.

Before we conduct the pre-conceptual design and establish the final layout that is appropriate to the domestic situation, we summarized the detailed configurations of the SARAF-PHASE2 (from injector to linac)and IFMIF/IFMIF-DONES (HEBT).

1. Electron Cyclotron Resonance Ion Source (ECR IS): SARAF adopts a 2.45 GHz normal-conducting (NC) ECR IS for H^+ and D^+ beam injection, and the output beam energy is 20 keV/u with 5 mA beam current. The output normalized RMS beam emittance is about 0.15 mm-mrad.
2. Low Energy Beam Transport (LEBT): The main function of LEBT line is the beam matching between ECR IS and RFQ. Three solenoids are used for the transverse focusing and one dipole magnet is installed for beam separation of different charge states.
3. Radio Frequency Quadrupole (RFQ): The SARAF RFQ is based on 4-rod structure (3.8 m long, 1.52 Kilpatrick) with 176 MHz operating frequency. The input and output beam energies are 20 keV/u and 1.27 MeV/u, respectively. The electrode voltage is 56 kV and the acceptance range of RF power is over 200 kW. The output normalized RMS beam emittances are about 0.2 mm-mrad in transverse and 0.12 MeV·deg in longitudinal space. Recently, a new 4-rod structure has been developed by Soreq Nuclear Research Center (SNRC) and implemented for SARAF-PHASE2 upgrade. In order to lower the RF power, they reduced the RFQ exit energy requirement from 1.5 MeV/u to 1.27 MeV/u [24, 25].
4. Medium Energy Beam Transport (MEBT): The main function of MEBT line is the beam matching between RFQ and super-conducting linac. Beam energy is 1.27 MeV/u. Because SARAF considers both CW and pulsed beam operations, additional space for beam chopping is needed (chopper, beam dump of the chopped beam during the commissioning, and beam diagnostic devices). Eight quadrupoles are installed; four for the basic transverse focusing and four for beam matching of the chopped beam along the extended MEBT line. Three rebunchers (176 MHz NC 3-gap, 28 cm long, copper-plated stainless steel) are used for longitudinal beam matching; two for the basic matching of longitudinal beam size and the additional one is for the pulsed beam matching [26]. There are two diagnostic boxes including Beam Position Monitor (BPM), AC Current Transformer (ACCT), and Beam Profile Chamber (BPC). Also, there are three H/V slit boxes and three sets of $x-y$ scrapers [27].
5. Super-conducting Radio Frequency (SRF) linac: The detailed component specifications of SRF linac section of the SARAF-PHASE2 are shown in Table 3 [28–30]. The 176 MHz super-conducting (SC) Half-Wave-Resonator (HWR) cavities are used for accelerating deuteron beams up to 40 MeV. The first two identical cryomodules house low-beta ($\beta_{opt} = 0.091$), 280 mm long (flange to flange) HWR cavities and the two identical last cryomodules house high-beta ($\beta_{opt} = 0.181$), 410 mm long (flange to flange) HWR cavities [11]. Here, β_{opt} is the optimal beta which maximizes the transit time factor T [28]. The effective length $L_{eff} = 2 \times (\beta_{opt}\lambda/2)$ and accelerating field $(E_0T)_{acc} = V_{acc}/L_{eff}$ of 2-gap RF cavities are defined at the optimal beta. Within one cryomodule, SC cavities and SC solenoid magnets are installed together, which makes the alignment much easier and the lattice period more compact. Also, the beam remains axisymmetric under the solenoid focusing channels.
6. High Energy Beam Transport (HEBT): The IFMIF/IFMIF-DONES HEBT line consists of eighteen quadrupole magnets and twelve steerer magnets for transverse focusing and centroid control. There are two bending magnets of 9° angle with quasi-achromatic condition to minimize upstream machine activation due to the neutron back-streaming from the target. Also, two duodecapoles and two octupoles are used to shape the beam

Table 3 Specifications of SARAF-PHASE2 SRF linac components

Cryomodule	1 &2	3 &4
β_{opt}	0.091	0.181
Cavity type	SC HWR	
# cavities/cryomodule	6, 7	7, 7
# total cavities	13	14
Frequency (MHz)	176	176
Flange to flange (m)	0.28	0.41
L_{eff} (m)	0.155	0.308
$(E_0T)_{acc}$ (MV/m)	6.5	7.5
Focusing magnet	SC solenoid	
# magnets/cryomodule	6	4
# total magnets	12	8
B max of magnet (T)	5.8	
Beam energy (MeV/u)	1.27 → 5.8	5.8 → 20
Beam current (mA)	5	
RF power per cavity (kW)	10	20
Temperature (K)	4.5	

suited for the required footprint in transverse directions. The non-linear multipole magnets and the subsequent quadrupole lattices make the beam uniformly distributed in x and y directions [20–22, 31]. A pair of octupoles has the influence on the beam uniformity and the shape of peak edges. A pair of duodecapoles only affects the beam particles at the far fringes, which has negligible effect on the beam core distributions. The target beam size can be manipulated by controlling the field strength of quadrupoles located after the multipole magnets and the length of drift space to the target. Because of the high space-charge effects, scrapers and lead shutters should be installed to protect duodecapoles from beam loss situations [32]. The HEBT line can be divided by three sections; Beam Transport Room (BTR), Radiation Isolation Room (RIR), and Target Interface Room (TIR) [33, 34]. The TIR is the last part of accelerator and plays the roles of beam diagnostics, stabilization, and alignment. Due to very high activation rates generated from (D-Li) reactions near the Target Cell (TC) room, lead shutters are installed before RIR-TIR wall, TIR-TC wall, and beam dump. Also, all the equipment in HEBT line is expected to be operated by 100% of Remote Handling (RH). Furthermore, beam pipe material is replaced by aluminum from SS316L to reduce the activation. The essential beam diagnostics devices in TIR include (1) BPM: to center the beam at target, (2) ACCT/DCCT: to measure the beam intensity, and tune the magnets and scraper apertures, (3) BPC: to monitor the required beam footprint at target, avoid $x-y$ coupling from non-linear magnetic fields, and tune the magnet strength. Beam dump line is bent by 30° and shielded by using lead shutter and concrete wall. A scraper at the end of HEBT is needed to limit the beam halo impact on the beam dump entrance. The beam dump has a copper cone structure to maximize the shielding efficiency [35].

5 Pre-conceptual design

Through an overall case study, as well as comparison and analysis of the detailed specifications of the existing or planned facilities over the world, it is possible to create a conceptual diagram for a deuteron-dedicated linac which is suitable for the Korean domestic fusion research program. Figure 1 shows the final expected layout of the D^+ linac.

1. ECR IS: A high-current deuteron beam can be produced from ECR IS, in which the two solenoids make a mirror field to confine the ECR plasma axially, while the hexapole magnet confines the plasma radially. Then, the potential difference between two electrodes is responsible for the extraction and acceleration of the ions. The ECR IS of SARAF case uses 2.45 GHz frequency, which does not require the hexapole magnets. A similar type of 2.45 GHz ECR IS is commercially available from PANTECHNIK or D-Pace. It is optimized for H^+, D^+, and T^+ ions and the performance guarantees beam inten-

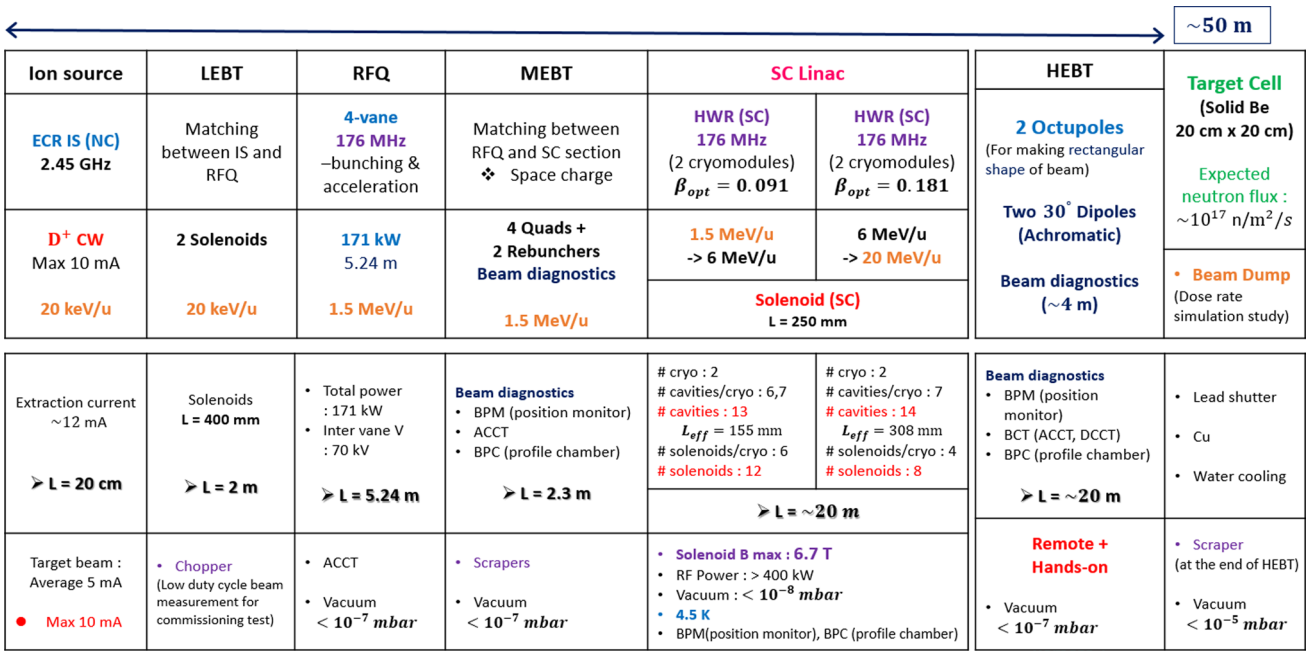

Fig. 1 Pre-conceptual design layout of the KFE D^+ linear accelerator for generating fusion-like neutrons

sity of 40 mA for proton and maximum 60 keV beam energy. For our pre-conceptual design, the extracted D^+ beam should have 20 keV/u of energy and around 12 mA of beam current, so that we can eventually get the maximum beam current of 10 mA even in the presence of the beam loss.

2. LEBT: The proposed linac will be operated with single ion species (i.e., deuteron only). Hence, a dipole magnet for injecting different ion species into the LEBT beamline is not necessary. Two NC solenoids are used to focus the transverse beam size and match the beam into the RFQ. The additional concern is that a chopper would be needed for low-duty cycle beam measurement during the beam commissioning period and for machine protection.
3. RFQ: The purpose of RFQ is beam bunching and low-energy acceleration. We accepted 4-vane type RFQ because of the higher beam power operational plan. Compared to 4-rod structure, the 4-vane type is known to be more suitable for the higher power load with lower power loss. The output beam energy from RFQ is set 1.5 MeV/u for the 20 keV/u of input energy. A 176 MHz RF frequency has been chosen following the SARAF design specifications.
4. MEBT: In the MEBT line, we do not need any additional space for beam chopping, as only the CW operation is envisioned. For the beam matching between RFQ and SRF linac section, at least four quadrupole magnets and two rebunchers are required for focusing the beam in the transverse and longitudinal directions, respectively. Beam diagnostics in the MEBT line should be considered such as BPM, ACCT, and BPC. Also, a couple of scrapers can be used to suppress the beam loss situations generated from high space-charge forces.
5. SRF linac: Our target beam specification is 400 kW beam power of CW mode. Therefore, a SRF linac is the best choice because almost 100% of RF power can be delivered to the beam itself and the power dissipation on the cavity wall is not a limiting issue. However, a sophisticated system to keep the helium cooling pressure very stable with the temperature of 4 K or 2 K is highly required. In general, an ideal synchronous particle velocity of the deuteron-dedicated accelerator is larger than that of heavy ion beams. In that sense, Half-Wave Resonator (HWR) is more suitable for the SC cavity structure than Quarter-Wave Resonator (QWR). The resonance frequency of the cavity is 176 MHz following the RFQ frequency, which is based on the SARAF design specifications. The total power for our SRF linac is over 400 kW. It means that we need more power suppliers and higher-power RF couplers than those of SARAF-PHASE2. There are four cryomodules (two for low $\beta_{\mathrm{opt}} = 0.091$ and two for high $\beta_{\mathrm{opt}} = 0.181$). SC solenoids are used for transverse beam focusing, which will be installed within the SC cryomodule together with RF cavities. It makes easier alignments along the periodic lattices and the beam remains axisymmetric under the solenoid focusing lattice. As shown in Fig. 1, the numbers of cavities and solenoids per cryomodule are the same with SARAF-PHASE2 cases (see also Table 3), and more detailed specifications will be covered from preliminary simulation study in the next section.
6. HEBT: After the beam is accelerated up to 40 MeV, we should make the beam having a rectangular-shaped uniform density profile in transverse plane. This can be achieved by using two octupole magnets and an elaborate arrangement of quadrupole magnets between the octupoles and target. In general, octupole field strength and the beam phase advance from octupole to target determine the central uniformity of particle distributions [31]. Duodecapoles affect the particles at far fringes and have negligible effect on the beam core density. The large space-charge forces can excite the non-uniform halo formations at the far fringe region and it can be manipulated by using duodecapoles to keep the sharp edge shape at target. However, in our pre-conceptual design study, we do not consider duodecapoles because it has been found that the duodecapoles do not affect the beam uniformity for the relatively low beam current cases (≤ 10 mA). Also, we decided to bend the beam line with two 30° bending magnets, so that the radiation effects on the accelerator components from the D-Li nuclear reactions at the target can be minimized. Preliminary simulation studies to implement the achromatic bending structure and uniform target beam generation along the HEBT line will be covered in the next section. Beam diagnostics are essential in the last part of the HEBT for optimizing the non-linear magnets. BPM is used for centering the beam at the target and tuning the magnets, ACCT (or DCCT) is used for checking the beam intensity, and BPC is used for achieving the required beam footprint at the target and tuning the magnetic field strength to avoid $x-y$ coupling from non-linear magnets. The last part of the HEBT line before the target room will be handled by both remote control and hands-on maintenance, which has been decided according to the calculation results of neutron radiation rates coming from neutron back-streaming at the target. Furthermore, detailed design configurations of shielding structures including lead shutter and concrete wall between the beamline and target room will be studied in the near future.
7. Target cell/Beam dump: Our target will be made of solid Be with 22 cm × 22 cm cross section. We expect that the neutron flux over 10^{17} n will be yielded when the 40 MeV deuteron beams hit the Be target. Then the gen-

erated neutrons are applied for breeding blanket component experiments or fusion material irradiation tests. Besides the beamline that is connected to the target cell, a beam dump line will be constructed. The fundamental material adopted in many beamline facilities to stop the high power ion beams is Cu. A detailed design of shielding system around the dump line should be made.

6 Preliminary start-to-end simulation

According to the results of pre-conceptual design study reported in the previous section, we have done the preliminary start-to-end simulation. The beam dynamics/optics calculations are essential to review the target beam availability and validate the device specifications.

6.1 ECRIS

An ECR ion source is often used in proton and heavy-ion accelerators to produce intense beams of positive ions. One of the main goals of ECR ion source design consideration is to produce high current beams while keeping transverse emittance as low as possible. To prevent emittance growth, pentode extraction electrodes are designed using the code IBSimu [36]. We applied optimum potential values and 3D magnetic field maps calculated for the system using Radia. The design parameters (see Table 4) are selected to meet the beam requirements for the RFQ, such the required input energy, acceptable normalized emittance, and desired beam current.

Figure 2 illustrates ion beam trajectory with the five-electrode simulation configuration consisting of a plasma electrode, a puller electrode, two ground electrodes, and a negative electrode on a two-dimensional cylindrical symmetry geometry. The extraction system producing 10 mA D^+ beam at 40 keV final beam energy (or, 20 keV/u) has been simulated with IBSimu.

The plasma generation occurs in correspondence with the resonant magnetic field. The amplitude of the energy absorption is proportional to the electromagnetic field orthogonal to the magnetostatic field [37]. The ECR condition is expressed by the well-known formula:

$$\omega_{\mathrm{RF}} = \frac{q_{\mathrm{e}} B_{\mathrm{ECR}}}{m_{\mathrm{e}}}, \tag{1}$$

where ω_{RF} is the microwave angular frequency, q_{e} the electron elementary charge, B_{ECR} the magnetic field at the resonance, and m_{e} the electron mass. For our 2.45 GHz ECRIS, double magnet coils are adopted and the ECR zone magnetic field is determined by the above formula. The maximum mirror magnetic field is calculated to be 0.275 T according to $B_{\mathrm{inj}}/B_{\mathrm{min}} \sim 3.76$ injection condition.

Extraction electrodes witness half of the mirror magnetic field (see Fig. 2) As a result, the effect of the magnetic field on beam parameters could be observed. Beam distributions are compared for cases with and without applying a magnetic field on electrodes (see Table 5). When B-field is applied on extraction electrodes both current and normalized-emittance values are increased but not significantly.

Table 4 Design parameters of ECR IS

Frequency	2.45 GHz
Ion	D^+
Ion current	10 mA
Extraction energy	20 keV/u
$\epsilon_{\mathrm{Norm,RMS}}$	< 0.2 mm-mrad
Operation mode	CW

Table 5 Effects of half mirror magnetic field on extraction process

	With B field	Without B field
$\epsilon_{\mathrm{Norm,RMS}}$ (mm-mrad)	0.091	0.084
Ion current (mA)	10.2	10

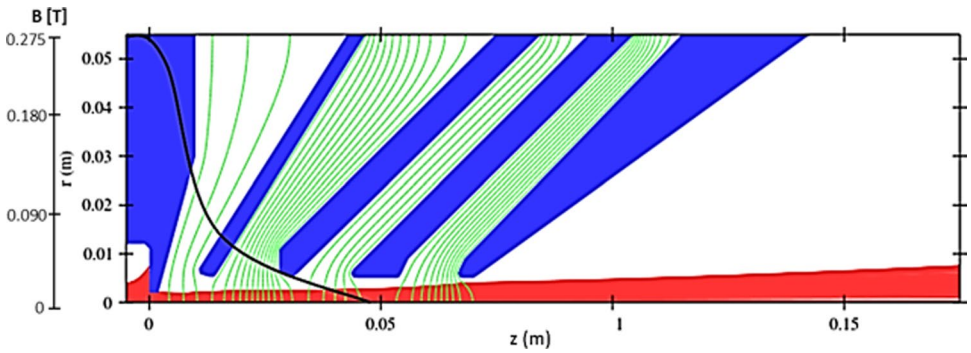

Fig. 2 This graph shows five-electrodes (blue shapes) extraction system. D^+ beams (red) are created inside the plasma electrode and extracted along the propagation axis with around 10 mA of beam current. A half mirror magnetic field (black line) is applied to electrodes. Green lines indicate the equipotential surfaces

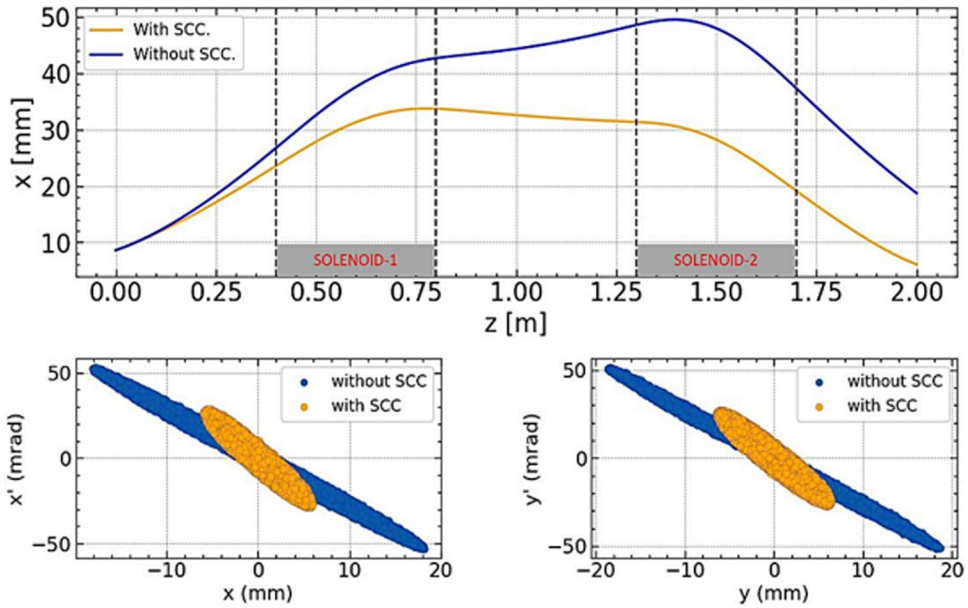

Fig. 3 Horizontal beam envelopes are shown with SCC (orange line) and without SCC (blue line). Graphs below show the horizontal and vertical phase spaces of the D^+ beam at the exit of the LEBT with a 10 mA beam current

6.2 LEBT

The LEBT is primarily responsible for matching the beam's optical functions between the ion source and the RFQ. In this study, the LEBT system transports the D^+ beam at 40 keV and 10 mA from the ECR ion source to the RFQ entrance with two NC solenoid magnets. We conducted beam transport simulations through the LEBT including the influences of space charge using the Warp code. The Warp code developed for heavy ion-driven inertial fusion energy studies, has been widely used to model high-intensity ion (and electron) beams and plasmas [38].

In order to transport medium to high-intensity low-energy ions, space charge compensation (SCC) is often essential. A space charge is generated by the charges of the beam ions themselves, and the associated electric self-field defocuses the beam. In the simplest model, the space charge compensation can be expressed in the form of a space charge compensation factor f_e, reducing the total beam current I_b as follows [39]:

$$I_b \rightarrow I_b(1 - f_e). \tag{2}$$

In the Warp code initial beam distributions at the exit of the ECR ion source were loaded A K-V beam distribution has been assumed, in which the effective (total) emittance is four times the RMS beam emittance. The second step of the simulation will involve predicting the space charge compensation factor considering Coulomb collisions between the primary beam ions and the compensating electrons self-consistently.

Figure 3 illustrates the horizontal beam distribution along the 2-m-long LEBT line, which consists of two solenoid magnets. It is seen that the beam radius is reduced after the space charge compensation method is applied. Besides, the horizontal and vertical RMS normalized beam emittances are compared at the exit of LEBT (see Table 6).

Table 6 Beam emittance comparison at the end of LEBT

	No SCC	With SCC
$\epsilon_{\mathrm{Norm,RMS},x}$ (mm-mrad)	0.169	0.094
$\epsilon_{\mathrm{Norm,RMS},y}$ (mm-mrad)	0.123	0.099

Table 7 Main design parameters of the RFQ

Ion type	D^+
RFQ type	4-vane
Operating mode	CW
Ion current (mA)	10
RF frequency (MHz)	176
Inter-vane voltage (kV)	70
Input $\epsilon_{\mathrm{Norm,RMS}}$ (mm-mrad)	< 0.2
Input energy (keV/u)	20
Output energy (MeV/u)	1.5
Average aperture radius (cm)	0.42
Synchronous phase	− 90° to − 30°

6.3 RFQ

The proposed RFQ operates at a frequency of 176 MHz and accelerates a 10 mA deuterium beam from 40 keV to 3 MeV. Basic design and beam dynamics studies were performed assuming a 4D waterbag input beam distribution

with 105 macro-particles using the standard codes Parmteq [40] and Toutatis [41] (Table 7).

A major objective of the design of RFQ is to maximize longitudinal acceptance and transmission efficiency, while simultaneously minimizing longitudinal and transverse emittance growths, beam losses, and vane length. The input beam energy is chosen in order to balance the RFQ length and the space-charge effects. A low-energy input beam makes the RFQ shorter, whereas an input beam with high energy minimizes the effects of space charge. As a result, we choose 20 keV/u as the input energy for the RFQ design. A high inter-vane voltage results in a high accelerating gradient, which makes the RFQ shorter. However, it requires more RF power dissipation per unit length and increases the risk of RF breakdown [42]. To ensure reliable operation of the RFQ, 70 kV inter-vane voltage is selected based on operational experiences (Fig. 4).

A benchmarking of the beam dynamics design was conducted using the Toutatis code. Table 8 shows that the beam transmission efficiency for 523.5 cm vane length provided by Toutatis is 98.65%, slightly lower than the value of 98.70% provided by Parmteq. This discrepancy is likely due to the different particle loss criteria used in the two codes. In Toutatis, a particle is declared lost when it hits the pole surface, whereas, in Parmteq, a particle is declared lost when it leaves a square area with an edge equal to two times the minimum aperture [16]. The transverse and longitudinal beam distributions at the end of the RFQ cell are given in Fig. 5 and obviously, both codes agree reasonably well.

6.4 MEBT

Figure 6 shows simulation results of the MEBT line by using TraceWin multi-particle simulation code [43]. There are four quadrupole magnets and two 3-gap type rebunchers to focus the transverse and longitudinal beam sizes, respectively. The initial beam parameters are based on the output beam parameters from RFQ and the output beam is matched into the super-conducting linac. Here, the length of quadrupole magnets is 15 cm and the magnetic field strength is 27, – 13, 9, – 13 T/m, each. The length of the rebunchers is 20.4 cm and the accelerating voltage is 94 and 151 kV, each. The empty space for beam diagnostics is set to be 50 cm and the total length of the MEBT line is 2.3 m.

6.5 SRF linac

After passing through the MEBT line, the matched beam is transported along the super-conducting cavities and solenoid focusing channel. Figure 7 shows simulation results of the SRF linac. Under the solenoid focusing lattice, the beam is axisymmetric as shown in Fig. 7a. Deuteron beam is accelerated from 1.5 to 6 MeV/u through cryomodules 1 and 2 of low $\beta_{opt} = 0.091$ region, and to 20 MeV/u through cryomodules 3 and 4 of high $\beta_{opt} = 0.181$ region. It is considered that the free space between the two cryomodules is set to be 31 cm for the beam diagnostic boxes and vacuum pump. The solenoid package is including a 25 cm solenoid, upstream BPM at each solenoid, magnet steerer, end bellow, and flanges. The detailed specifications according to

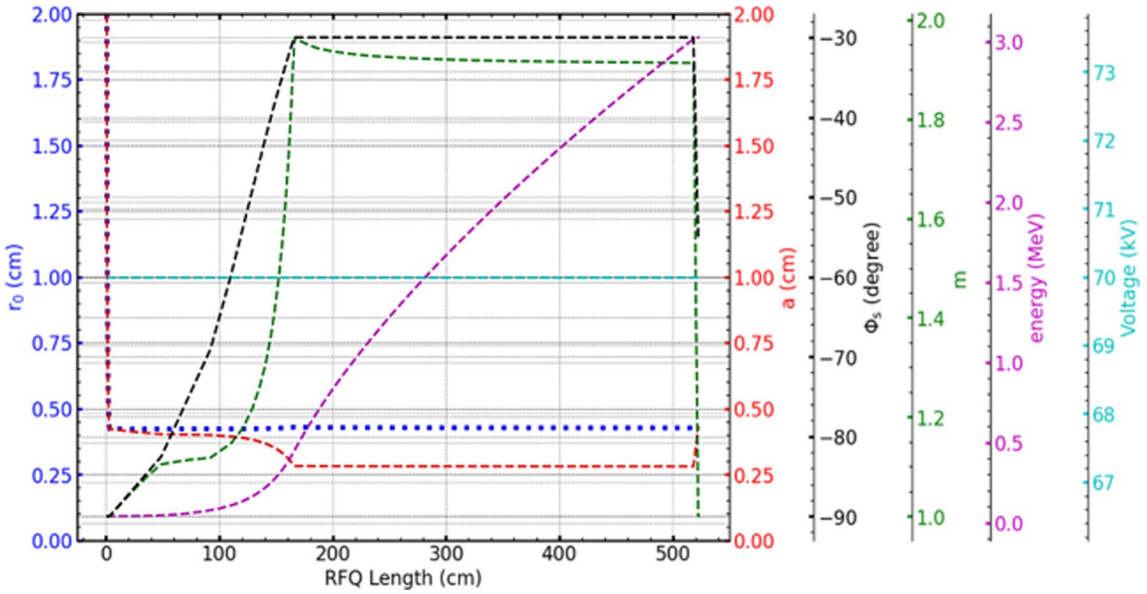

Fig. 4 The final RFQ design parameters. Here, r_0 is the average aperture, a is the minimum aperture, ϕ_s is the synchronous phase, and m is the modulation factor. The energy value is the kinetic energy of the synchronous particles and voltage value is the inter-vane voltage between opposite electrodes

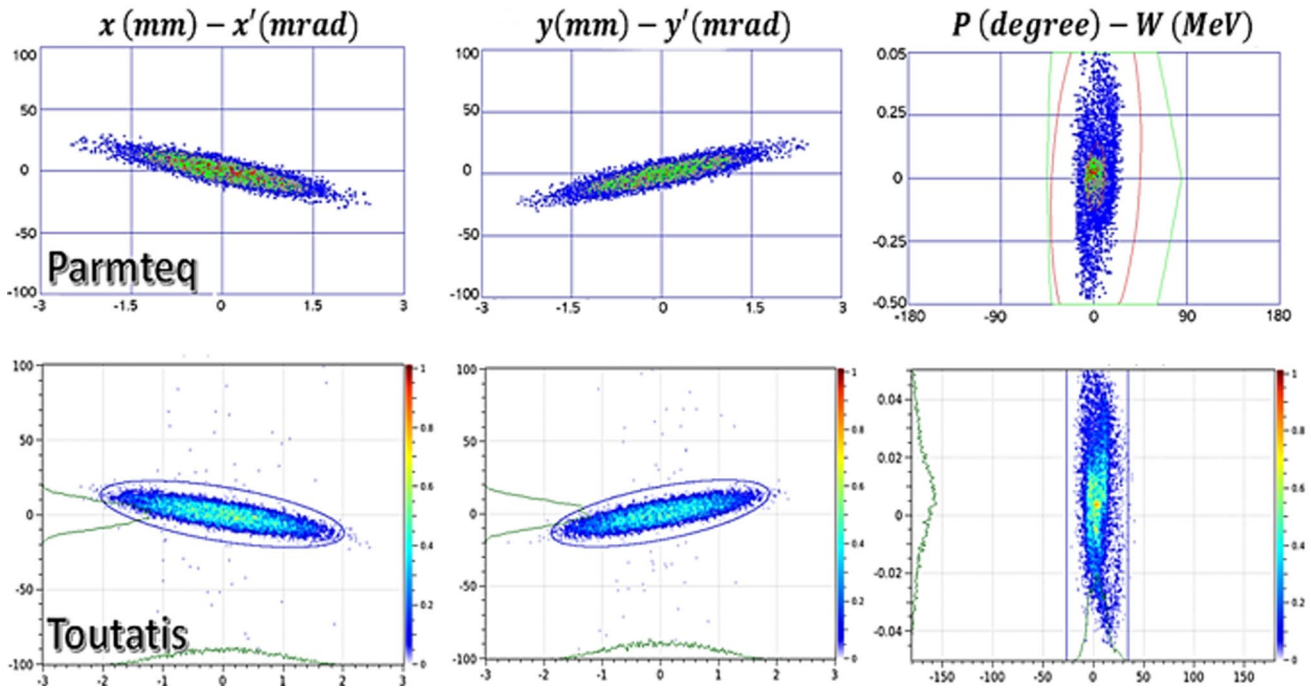

Fig. 5 Output particle distributions (top: from Parmteq, bottom: from Toutatis)

Table 8 Comparison of Parmteq and Toutatis simulations

	$\epsilon_{x,\mathrm{Norm}}$ (mm-mrad)	$\epsilon_{y,\mathrm{Norm}}$ (mm-mrad)	$\epsilon_{z,\mathrm{Norm}}$ (MeV-deg)	Transmission rate (%)	Length (cm)
Parmteq	0.21040	0.21310	0.10815	98.70	523.5
Toutatis	0.20852	0.21494	0.12902	98.65	523.5

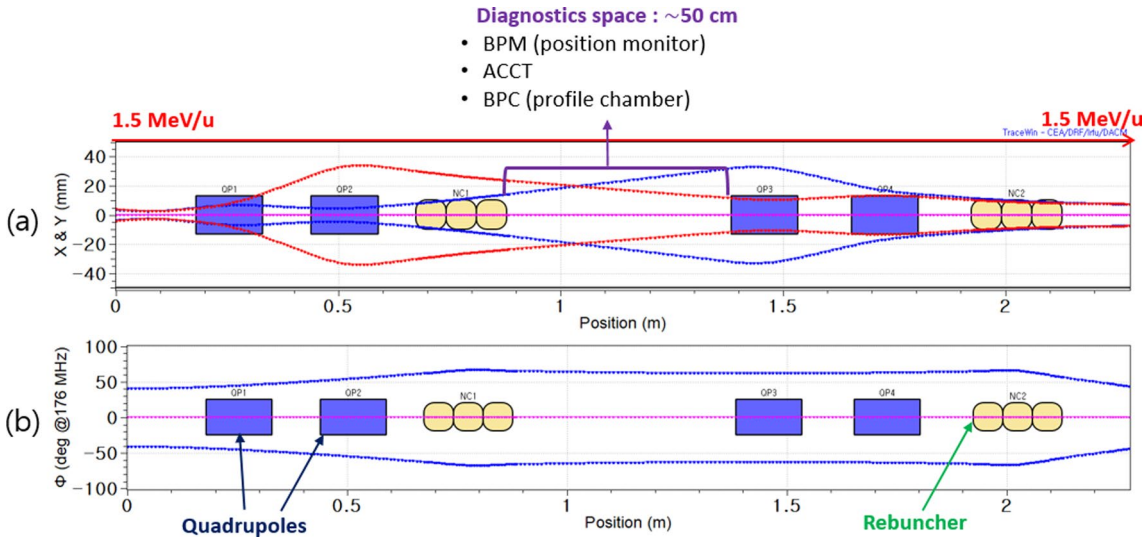

Fig. 6 Simulation results of MEBT line. **a** Horizontal (x) and vertical (y) beam envelope sizes (mm), and **b** longitudinal phase (deg) along the MEBT line for matching the beam between the RFQ and SRF linac

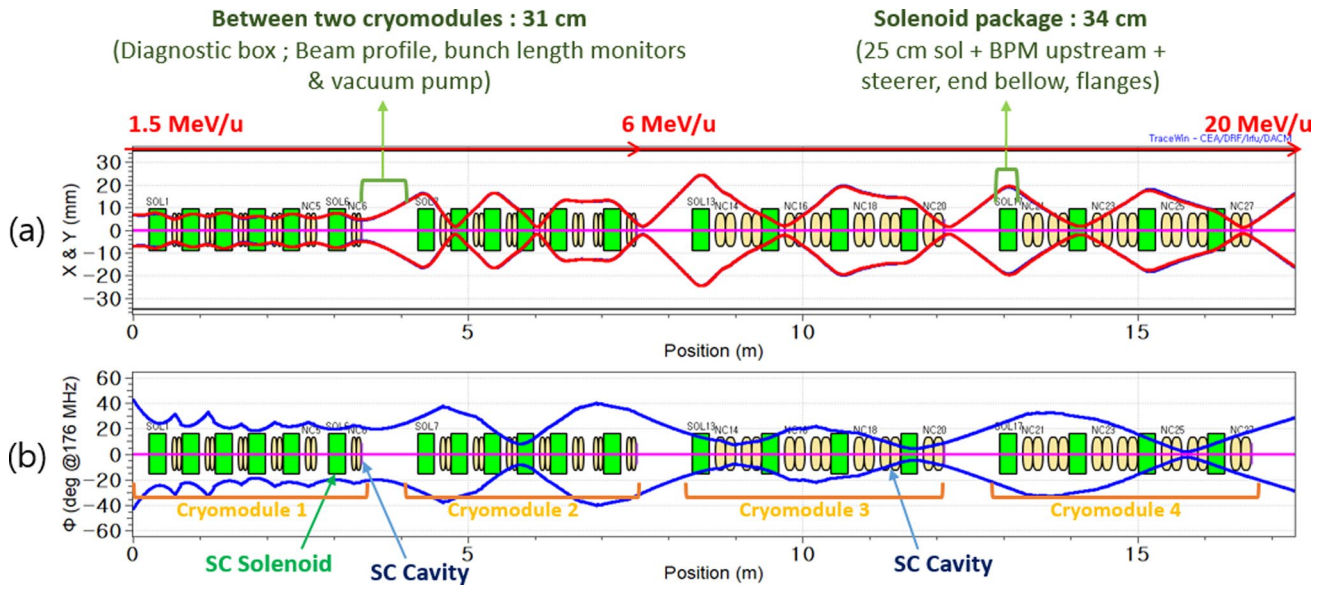

Fig. 7 Simulation results of SRF linac. **a** Horizontal (x) and vertical (y) beam envelope sizes (mm), and **b** longitudinal phase (deg) along the SRF linac with initially well-matched condition

the simulation results are summarized in Table 9. The beam pipe bore diameters are 36 mm in the low beta section and 40 mm in the high beta section.

6.6 HEBT

Figure 8 shows simulation results of the HEBT line that leads to the target cell. There are fourteen quadrupole magnets, two dipole magnets (30° achromatic), and two octupole magnets. The five quadrupole magnets between the octupoles and the target are aligned to make a rectangular-shaped beam with a uniform density profile. The magnetic field strengths of the quadrupoles and two octupoles are adjusted for achieving the optimized target beam generation. As a result of the simulation studies, the octupole magnetic field strengths are optimized to be -3600 and 1280 T/m^3 with 1.3 m length of the interval between the two octupoles. The maximum field gradient of quadrupoles is 12 T/m. In the last section of the HEBT, we consider the beam diagnostics space for about 4 m long and the final total length of the HEBT line is about 20 m.

The final beam distributions on different phase-space planes are shown in Fig. 9. The number of macro-particles used in the TraceWin simulation code is 100,000. Figure 9a, b show the beam density on x–x' and y–y' (mm-mrad) planes, respectively. As the octupole field strength increases, the central flat-top uniformity of the beam increases while the spikes at the beam tail become larger. By optimizing the quadrupole lattice design, the final beam uniformity can be improved. The length of drift space before the target would affect the size of the beam footprint at the target. Also, the final target beam requirements will be defined, which is optimized for our design target structure. The deuteron irradiation studies will be done by considering the amount of generated neutron flux and the acceptable range of heat and thermal stress on Be target. The more detailed studies for HEBT beam line optimization for the generation of uniform density beam on the target is in progress and will be reported elsewhere.

Table 9 Specifications of SRF linac components according to the preliminary simulation results

Cryomodule	1 &2	3 &4
β_{opt}	0.091	0.181
Cavity type	SC π-mode two-gap cavity	
# cavities/cryomodule	6, 7	7, 7
# total cavities	13	14
Frequency (MHz)	176	176
L_{eff} (m)	0.155	0.308
Focusing magnet	SC Solenoid	
# magnets/cryomodule	6	4
# total magnets	12	8
B max of magnet (T)	6.7	
Beam energy (MeV/u)	1.5 → 6	6 → 20
Beam current (mA)	10	
RF power per cavity (kW)	20	40
Temperature (K)	4.5	

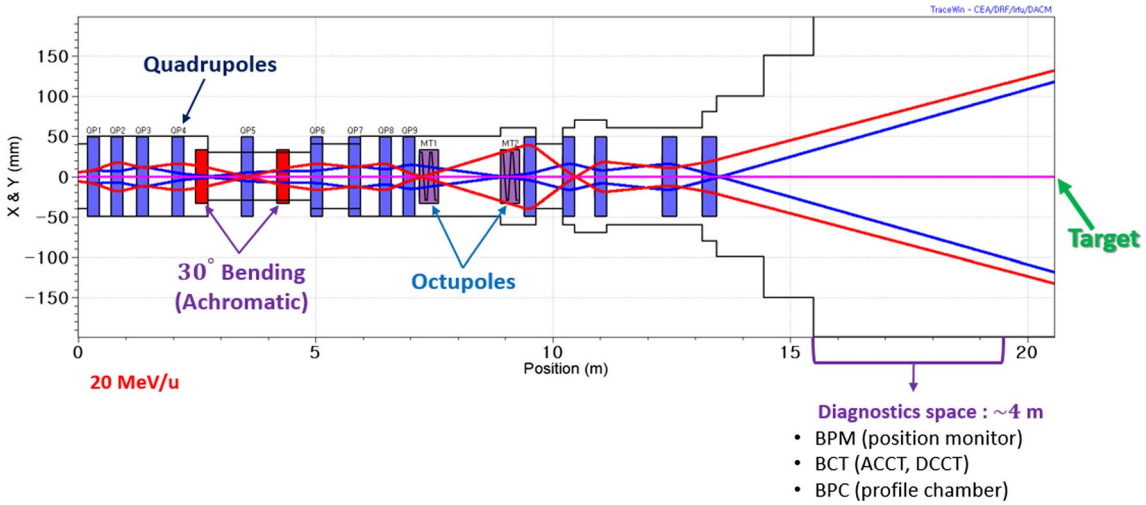

Fig. 8 Simulation results of HEBT line. Horizontal (x) and vertical (y) beam envelope sizes (mm) along the HEBT line for matching the beam between SRF linac and target facility

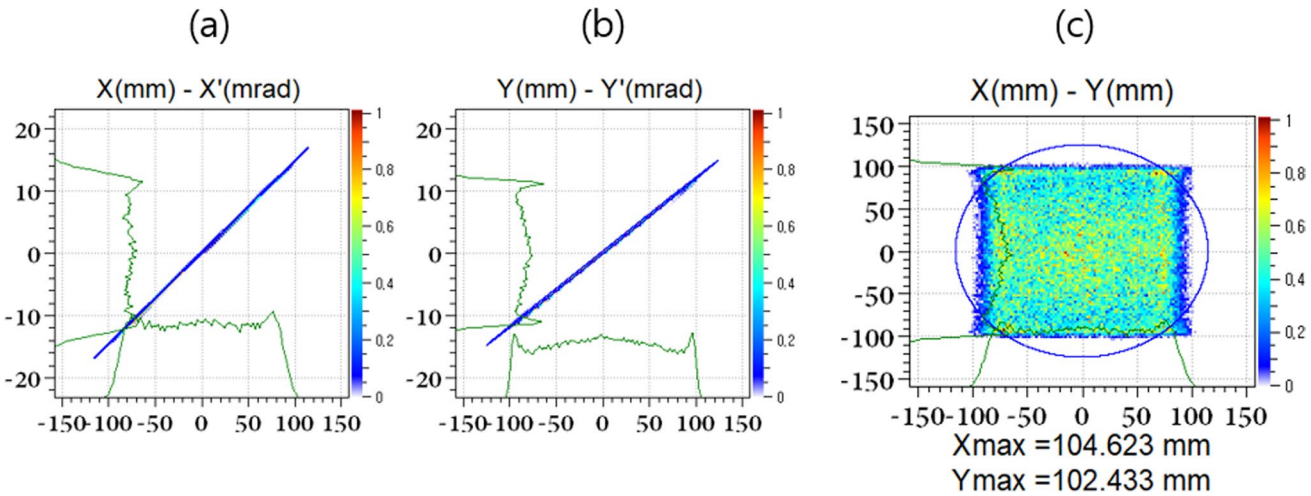

Fig. 9 Beam distributions at the target on different phase spaces. Density profile on **a** x–x' (mm-mrad), **b** y–y' (mm-mrad), and **c** x–y (mm-mm) phase planes. The particles are uniformly distributed within a rectangular shape of 20 cm × 20 cm cross section

7 Outlook and discussion

Neutron irradiation experiments with relatively low energy (~ 40 MeV) and high average current D^+ accelerators are being pursued worldwide for the studies of blanket structural materials, divertor functional materials, tritium release modules of DEMO, etc. To keep up with such trends in a timely manner, Korean fusion and accelerator communities should look into the best options for the domestic fusion engineering program. A dedicated tritium breeding unit test facility with a moderate-intensity (say, 10 mA) D^+ accelerator might be a reasonable option in terms of niche marketing or a mid-entry strategy. Hence, in this work, we present the case study, pre-conceptual design, and major component specification overview for developing such an accelerator. Preliminary beam dynamics and optics calculations suggest that there is no immediate showstopper from the accelerator physics point of view. Accelerator technology seems rather mature, whereas target design and neutronics appear rather challenging. Based on this work, a more complete conceptual design is being planned, which will provide viable input to the Korean fusion engineering road map.

Acknowledgements This work was supported by Korea Institute of Fusion Energy (KFE) funded by the Government funds (Grant no. R &D/2022-CN2201-2 and KFE-CN2301).

References

1. Fact sheet: developing a bold vision for commercial fusion energy (The White House Press Releases, 2022)
2. H. Han, S. Park, C. Sung, J. Kang, Y. H. Lee, J. Chung, Y. S. Na, et al., A sustained high-temperature fusion plasma regime facilitated by fast ions. Nature **609 (7926)**, 269–275 (2022)
3. J. Knaster, Y. Okumura, Accelerators for fusion materials testing. Rev. Accel. Sci. Technol. **8**, 115 (2015)
4. J. Knaster, A. Moeslang, T. Muroga, Materials research for fusion. Nat. Phys. **12**, 424 (2016)
5. W. Krolas, A. Ibarra, F. Arbeiter, F. Arranz, D. Bernardi, M. Cappelli et al., The IFMIF-DONES fusion oriented neutron source: evolution of the design. Nucl. Fus. **61**, 125002 (2021)
6. S. Cho, *Technical gaps between HCCR TBM and DEMO blanket and their facilities development/plans, 1st iFPC* (Jeju, Korea, 2022)
7. S. Hong, S. Kwon, M. Ahn et al., *Neutronics analysis for conceptual design of target system based on a deuteron accelerator-driven fusion neutron source, 32nd SOFT* (Dubrovnik, Croatia, 2022)
8. T. Junquera, The SPIRAL2 project: construction progress and recent developments on the SC linac driver. In *13th International Conference on RF Superconductivity (SRF 2007). Joint Accelerator Conferences Website* (2007). pp. 35–41
9. E. Petit, Progress of the SPIRAL2 project. In *2nd International Particle Accelerator Conference (IPAC2011)* (2011). pp. 1912–1916
10. P. Dolegieviez, R. Ferdinand, X. Ledoux, H. Savajols, F. Varenne et al., Status of the SPIRAL2 project. In *Proceedings of 10th International Particle Accelerator Conference (IPAC'19)* (2019). pp. 844–847
11. N. Pichoff, P. Bredy, G. Ferrand, P. Girardot, F. Gougnaud, M. Jacquemet, A. Mosnier, P. Bertrand, M. Di Giacomo, R. Ferdinand et al., The SARAF-linac project for SARAF-Phase 2. In *Proceedings* of *6th International Particle Accelerator Conference (IPAC'15)* (2015). pp. 3683–3685
12. N. Pichoff, N. Bazin, D. Berkovits, D. Chirpaz-Cerbat, R. Cubizolles, M. Di Giacomo, J. Dumas, R. Duperrier, G. Ferrand, B. Gastineau et al., The SARAF-LINAC project 2017 status. In *Proceedings of 8th International Particle Accelerator Conference* (*IPAC'17)* (2017)
13. P. Garin, M. Sugimoto et al., Main baseline of IFMIF/EVEDA project. Fus. Eng. Des. **84**, 259 (2009)
14. S. Ishida, P. Cara, H. Dzitko, A. Kasugai, K. Sakamoto et al., Progress of IFMIF/EVEDA project and prospects for A-FNS. In *19th International Conference on RF Superconductivity (SRF2019)* (Dresden, Germany, 2019)
15. A. Ibarra, F. Arbeiter, D. Bernardi, M. Cappelli, A. Garcia, R. Heidinger, W. Krolas, U. Fischer, F. Martin-Fuertes, G. Micciché et al., The IFMIF-DONES project: preliminary engineering design. Nucl. Fusion **58**, 105002 (2018)
16. W.-P. Dou, W.-L. Chen, F.-F. Wang, Z.-J. Wang, C.-X. Li, Q. Wu, C. Wang, W.-S. Wang, H. Jia, P. Zhang et al., Beam dynamics and commissioning of CW RFQ for a compact deuteron-beryllium neutron source. Nucl. Instrum. Methods Phys. Res. Sect. A: Accel. Spectrom. Detect. Assoc. Equip. **903**, 85 (2018)
17. N. Lecesne, C. Eleon, C. Feierstein, G. Gaubert, Y. Huguet, P. Jardin, F. Lemagnen, R. Leroy, J. Pacquet, F. Pellemoine et al., The radioactive ion beam production systems for the SPIRAL2 project. Rev. Sci. Instrum. **79**, 02A907 (2008)
18. M. Tessler, M. Paul, T. Palchan, S. Halfon, L. Weissman, N. Hazenshprung, A. Kreisel, T. Makmal, A. Shor, I. Silverman et al., Nucleosynthesis reactions with the high-intensity SARAF-LiLiT neutron source. In *Proceedings of "The 26th International Nuclear Physics Conference", PoS (INPC2016)*, vol. 139 (2017)
19. I. Mardor, O. Aviv, M. Avrigeanu, D. Berkovits, A. Dahan, T. Dickel, I. Eliyahu, M. Gai, I. Gavish-Segev, S. Halfon et al., The Soreq applied research accelerator facility (SARAF): overview, research programs and future plans. Eur. Phys. J. A **54**, 1 (2018)
20. J. Knaster, A. Ibarra, J. Abal, A. Abou-Sena, F. Arbeiter, F. Arranz, J. Arroyo, E. Bargallo, P. Beauvais, D. Bernardi et al., The accomplishment of the engineering design activities of IFMIF/EVEDA: the European-Japanese project towards a Li (d, xn) fusion relevant neutron source. Nucl. Fusion **55**, 086003 (2015)
21. P. Nghiem, N. Chauvin, M. Comunian, O. Delferriere, R. Duperrier, A. Mosnier, C. Oliver, W. Simeoni, D. Uriot, Dynamics of the IFMIF very high-intensity beam. Laser Part. Beams **32**, 109 (2014)
22. C. Oliver, P. Cara, N. Chauvin, A. Gallego, and A. Ibarra, Phase-space transformation for a uniform target irradiation at DONES. In *28th International Linear Accelerator Conference* (2016). p. TUPRC006
23. K.-W. Tao, Y.-L. Zhang, H.-J. Cai, G. Yang, S. Zhang, X.-C. Zhang, Y. Yang, P. Lin, L.-W. Chen, X.-S. Yan et al., Simulation studies of the granular flow beryllium target for the compact materials irradiation facility. Nucl. Instrum. Methods Phys. Res. Sect. A Accel. Spectrom. Detect. Assoc. Equip. **942**, 162401 (2019)
24. A. Perry, D. Berkovits, H. Dafna, B. Kaizer, Y. Luner, J. Rodnizki, A. Shor, I. Silverman, R. Duperrier, G. Ferrand et al., Comissioning of the new SARAF RFQ and design of the new linac. In *29th Linear Accelerator Conference (LINAC'18), (Shanghai, China)* (2018)
25. L. Weissman, A. Perry, A. Bechtold, D. Berkovits, B. Kaizer, Y. Luner, P. Niewieczerzal, J. Rodnizki, I. Silverman, A. Shor et al., Installation, high-power conditioning and beam commissioning of the upgraded SARAF 4-rods RFQ. J. Instrum. **13**(05), T05004
26. L. Zhao, X. Zhu, J. Dumas, D. Chirpaz, T. Joannem, F. Gohier, N. Solenne, P. Guiho, R. Braud, O. Piquet et al., Study and test of the rebuncher for SARAF-linac phase II. Nucl. Instrum. Methods Phys. Res. Sect. A: Accel. Spectrom. Detect. Assoc. Equip. **986**, 164716 (2021)
27. P.A.P. Nghiem, B. Dalena, J. Dumas, N. Pichoff, D. Uriot et al., Strategy of beam tuning implementation for the SARAF MEBT and SC linac. In *Proceedings of 8th International Particle Accelerator Conference (IPAC'17), Copenhagen, Denmark, 2017* (JACOW, Geneva, Switzerland, 2017). pp. 652–654
28. G. Ferrand, N. Pichoff, Designing a 176 MHz superconducting half-wave resonator for SARAF-phase II-studies and results. IEEE Trans. Appl. Supercond. **32**, 1 (2022)
29. G. Ferrand, L. Boudjaoui, D. Chirpaz-Cerbat, P. Hardy, F. Leseigneur, C. Madec, N. Misiara, N. Pichoff et al., Design of the HWR cavities for SARAF. In *Proceedings of 7th International Particle Accelerator Conference (IPAC'16)* (2016). pp. 2119–2121
30. N. Pichoff, D. Chirpaz-Cerbat, R. Cubizolles, J. Dumas, R. Duperrier, G. Ferrand, B. Gastineau, F. Leseigneur, C. Madec, T. Plaisant et al., Discussion on SARAF-linac cryomodules. In *61st ICFA Advanced Beam Dynamics Workshop on High-Intensity and High-Brightness Hadron Beams* (2018). p. TUA2WC01
31. Y. Yuri, N. Miyawaki, T. Kamiya, W. Yokota, K. Arakawa, M. Fukuda, Uniformization of the transverse beam profile by means of nonlinear focusing method. Phys. Rev. Spec. Top. Accel. Beams **10**, 104001 (2007)
32. P. Nghiem, N. Chauvin, M. Comunian, O. Delferriere, R. Duperrier, A. Mosnier, C. Oliver, D. Uriot, The IFMIF-EVEDA challenges in beam dynamics and their treatment. Nucl. Instrum. Methods Phys. Res. Sect. A: Accel. Spectrom. Detect. Assoc. Equip. **654**, 63 (2011)

33. O. Nomen, D. Sanchez-Herranz, C. Oliver, I. Podadera, R. Varela, F. Ogando, V. Hauer, F. Arranz, S. Coloma, R. Heidinger et al., Preliminary design of the HEBT of IFMIF DONES. Fusion Eng. Des. **153**, 111515 (2020)
34. D. Sánchez-Herranz, O. Nomen, F. Arranz, S. Coloma, I. Podadera, R. Varela, Design of the HEBT components inside TIR room of the IFMIF DONES facility. Fusion Eng. Des. **168**, 112636 (2021)
35. O. Nomen, B. Brañas, F. Ogando, F. Arranz, P. Sauvan, J. Castellanos, Lead shutter for the IFMIF LIPAc accelerator. Nucl. Instrum. Methods Phys. Res. Sect. A: Accel. Spectrom. Detect. Assoc. Equip. **901**, 69 (2018)
36. T. Kalvas, O. Tarvainen, T. Ropponen, O. Steczkiewicz, J. Ärje, H. Clark, IBSimu: a three-dimensional simulation software for charged particle optics. Rev. Sci. Instrum. **81**, 02B703 (2010)
37. L. Neri, L. Celona, High stability microwave discharge ion sources. Sci. Rep. **12**, 1 (2022)
38. D.P. Grote, A. Friedman, J.-L. Vay, I. Haber, The Warp code: modeling high intensity ion beams. In *AIP Conference Proceedings*, vol 749 (American Institute of Physics, 2005). pp. 55–58.
39. D. Winklehner, D. Leitner, A space charge compensation model for positive DC ion beams. J. Instrum. **10**(10), T10006
40. K. Crandall, in *LANL Internal Report, Nr. LA-UR-96-1836* (2005)
41. R. Duperrier, Toutatis: a radio frequency quadrupole code. Phys. Rev. Spec. Top. Accel. Beams **3**, 124201 (2000)
42. S. Liu, Y. Wei, Y. Lu, Z. Wang, M. Han, T. Wei, Y. Xia, H. Li, S. Gao, P. Zheng, Development of a radio-frequency quadrupole accelerator for the HL-2A/2M tokamak diagnostic system. Appl. Sci. **12**, 4031 (2022)
43. D. Uriot, N. Pichoff et al., Status of TraceWin code. In *Proceedings of 6th International Particle Accelerator Conference (IPAC'15)*, **92** (2015)